Impact of Particle Aggregated Microbes on UV Disinfection. I: Evaluation of Spore–Clay Aggregates and Suspended Spores

Hadas Mamane[1] and Karl G. Linden, M.ASCE[2]

Abstract: Aggregation of microbes with particles can reduce the effectiveness of ultraviolet (UV) disinfection. This study evaluated the comparative impact of dispersed spores, dispersed spores mixed with clay particles (nonaggregated), spore–spore aggregates, and spore–clay aggregates on UV disinfection performance in simulated drinking waters. Aggregates were induced by flocculation with alum and characterized by particle size analysis (count, volume, and surface area) of dispersed and aggregated systems, scanning electron microscopy (SEM) and energy dispersive X-ray (EDX) analysis. It was concluded that spores within aggregates of the spore–clay system were protected from UV irradiation compared to nonaggregated spores and the difference between these systems was found to be statistically significant throughout the UV range tested. In addition SEM-EDX analysis suggested that aggregate composition is nonhomogeneous with respect to the ratio of spores and clay particles among aggregates. It was estimated that 30–50% of the spores in the aggregates tested were protected from UV irradiation.

DOI: 10.1061/(ASCE)0733-9372(2006)132:6(596)

CE Database subject headings: Microbes; Disinfection; Aggregates; Clays; Ultraviolet radiation; Water treatment.

Introduction

The impact of particles on ultraviolet (UV) disinfection has typically been studied by spiking turbidity and microbes into a sample water and contacting them via stirring, essentially measuring the effect of particle absorbance and scattering on UV performance. Passantino et al. (2004) concluded that clay turbidity up to 12 NTU, which is above the allowed turbidity limits for unfiltered water, did not affect the performance of UV disinfection of MS2. Of ultimate concern, however, is the impact of particle–microbe association on disinfection performance. According to the USEPA draft UV disinfection guidance manual (USEPA 2003) studies on the effect of turbidity on inactivation of microbes relate mainly to the scattering effect of disperse particles on UV irradiance, however these types of studies do not directly investigate the impact of particle–microbe association on UV. Therefore, studies in which microorganisms are spiked into a solution with particles or flocs not associated with each other, cannot substitute for studies that relate to microorganisms trapped within the floc network due to natural or induced flocculation. Templeton et al. (2003) found that MS2 virus aggregated within a floc prior to UV exposure resulted in 1-log reduction of MS2 inactivation compared to disperse particulate-free MS2. Malley (2000) investigated the effect of flocs collected from water and wastewater processes on MS2 disinfection by mixing those particles with the virus and concluded that different particles can effectively shield MS2 differently from UV inactivation. However MS2 was presumably protected due to shielding and not due to aggregation within the floc.

Aggregation and clumping have been shown to interfere with chemical disinfection of bacteria (Stewart and Olson 1996). Sobsey et al. (1991) showed that hepatitis A virus (HAV) associated with cells required tenfold the dose of free chlorine to achieve a 4 $\log_{10}$ inactivation compared to dispersed viruses. The effect of particles associated with microbes in wastewater is well established for UV disinfection (Parker and Darby 1995; Emerick et al. 1999, 2000) and it has been demonstrated that nonaggregated microbes in wastewater are easier to disinfect than aggregated ones. Aggregation of microbes with particles can result in reducing the effectiveness of UV disinfection by decreasing light through an aggregate due to absorption and scattering (Loge et al. 1999) and thus shielding microbes from UV light. Suspended particles in wastewater effluents can result in a higher UV demand because they can scatter and absorb UV light (Qualls et al. 1983).

In water treatment, the coagulation process is used to increase the rate of particle aggregation by transforming a stable suspension into an unstable suspension capable of aggregation. In conventional water treatment plants UV disinfection is applied usually after filtration or to unfiltered waters with low turbidity, however in some cases due to infrastructure constraints UV disinfection can be applied only to the raw or prefiltered waters. Disturbances in operation during filtration of flocculated aggregates in water, released from a filter breakthrough event, can negatively affect UV disinfection.

[1]Research Associate, Porter School of Environmental Studies and School of Mechanical Engineering, Tel-Aviv Univ., Tel-Aviv 69978, Israel.

[2]Associate Professor, Dept. of Civil and Environmental Engineering, Duke Univ., P.O. Box 90287, Durham, NC 27708-0287 (corresponding author). E-mail: kglinden@duke.edu

Note. Discussion open until November 1, 2006. Separate discussions must be submitted for individual papers. To extend the closing date by one month, a written request must be filed with the ASCE Managing Editor. The manuscript for this paper was submitted for review and possible publication on August 13, 2004; approved on October 12, 2005. This paper is part of the ***Journal of Environmental Engineering***, Vol. 132, No. 6, June 1, 2006. ©ASCE, ISSN 0733-9372/2006/6-596–606/ $25.00.

Researchers have shown that the threshold particle size beyond which coliform bacteria would be both associated with wastewater particles and protected from the UV disinfectant ranges between 7 and 10 μm (Cairns et al. 1993; Emerick et al. 1999), while coliform is 1×3 μm in size. For viruses this threshold particle size will likely be lower due to their smaller size, whereas for protozoans it will likely be larger. However not much is known about particles and microbe interactions in water during treatment and the impacts on UV disinfection. This study aimed to develop a better understanding and contrast the impact of microbe–particle aggregation and particle–microbe cosuspension on microbial inactivation by UV exposure. The initial goal was to produce a particle–microbe aggregate of montmorillonite clay particles with *Bacillus subtilis* spores suspended in simulated drinking water (DW) by addition of alum to the suspension of spores and clay particles using a jar test apparatus. Montmorillonite clay particles were chosen as a representative of natural inorganic particles in water sources (Passantino et al. 2004), while simulated DW was chosen to allow a controlled study through simulating surface waters. The specific objectives of this study were to (1) find conditions that were effective in formation of spore–spore or spore–clay aggregates suspended in simulated DW; (2) correlate measurements of particle size, and particle volume of spores cosuspended and aggregated with particles on flocculation performance; (3) compare the effect of disperse spores, spores cosuspended with clay particles (nonaggregated), spore–spore aggregates, and spore–clay aggregates on UV disinfection performance; (4) estimate aggregation efficiency and percent of spores within aggregates protected from UV; and (5) apply scanning electron microscopy to image spores and clay particles and differentiate them in aggregates using elemental analysis.

Materials and Methods

Experiments were performed using simulated DW at different pH values mixed with *B. subtilis* spores (a traditional pathogen surrogate microbe) and montmorillonite clay particles.

Bacillus Subtilis Spore Preparation and Enumeration

B. subtilis spores (ATCC 6633) were produced by a liquid cultivation technique and obtained freeze dried (Sommer and Cabaj 1993). Working solution was prepared by resuspending the spores in simulated DW as discussed below. Spore concentration was determined after serial tenfold dilutions of all the spore samples, followed by distributing 1 mL aliquots of the suspension on empty agar plates, pouring the agar medium (plate count agar) at 45°C into the plates (about 15–20 mL), and incubating 48±4 h at 37°C.

Clay Particle Preparation

The clay type used was SWy-2 which is Na-rich montmorillonite (Crook County, Wyo.) obtained from the Clay Minerals Society (Source Clays Repository). Clay particles were suspended in Millipore water at a concentration of ~1 g/100 mL. The suspension was placed in 100 mL graduated cylinders to allow the coarse particles to settle for 3 days (Tombacz et al. 1999). The supernatant collected from the cylinders by a pipette was centrifuged three times (Sorval Super T21, Asheville, N.C.), 15 min at 800 g, and the supernatant collected from centrifugation was used in the experiments (Stagg 1976). The Na–montmorillonite chemical composition was as follows: 63% SiO_2, 20% Al_2O_3, 3% Fe_2O_3, 2% K_2O and other impurities, while the cation exchange capacity was 76.4 meq/100 g. A detailed data sheet of the Na–montmorillonite chemical composition and characteristics can be obtained at ⟨http://www.clays.org/⟩ and Van Olphen and Fripiat (1979).

Simulated Drinking Water Preparation

The simulated drinking (SD) water characteristics were modeled after a natural surface water, and were developed to provide a consistent and controlled water quality over the period of the experiments. Three stock solutions were used to prepare experimental solutions. Two types of natural organic matter (NOM) used were obtained commercially, alginic acid (Sigma-Aldrich) and Suwannee River NOM (Averett et al. 1994, International Humic Substances Society ⟨www.ihss.gatech.edu⟩). These were, Stock A (4.84 mmol/L $NaNO_3$ and 113 mmol/L NaCl), Stock B (0.25 g/L NOM, Suwannee River from the International Humic Substances Society and 0.53 g/L alginic acid, pH 10, TOC=280 mg/L), and Stock C (0.1 mol/L KH_2PO_4). A combination of these stocks was diluted using deionized (DI) water with 0.1 mol/L NaOH, and spiked with 1.5 mmol/L $NaHCO_3$ (except pH 5) to prepare three waters at pH 5.0, 6.8, and 8.3 with a realistic level of dissolved inorganic carbon (Sharpless et al. 2003). *B. subtilis* spores at a concentration of 3×10^4 cfu/mL and clay particles at a concentration of 0, 5, and 10 NTU, with particle concentration of 8.08×10^7 and 1.27×10^8 for 5 and 10 NTU, respectively, were spiked into the waters with different pH levels. The chemical composition of the simulated waters obtained was as follows: 2.6 mg/L TOC, 5.3 mg/L alginic acid, 3 mg/L NO_3, 66 mg/L inorganic C as CO_2, 40 mg/L of Cl^-, and varying concentrations of PO_4^{-3}, K^+, and Na^+ according to the pH level. The alkalinity of water at pH 5, 6.8, and 8.2 (with 5 NTU clay) was 3, 111, and 156 mg/L as $CaCO_3$, respectively, the calcium carbonate concentration was 4 mg/L as $CaCO_3$, and conductivity was 550, 520, and 530 μS/cm, respectively.

Analytical Measurements

Measurements of zeta potential were performed with a zeta meter (model 3.0+ unit, Zeta-Meter Inc., Staunton, Va). Total organic carbon (TOC) was measured by a TOC analyzer (Tekmar, Dohrmann, Apollo 9000, Ohio). Turbidity was measured by turbidometer (Hach, model 2100N, Loveland, Colo.). Conductivity (APHA, Method 2510A) and pH (APHA, Method 4500-H) were measured via probes. Alkalinity (APHA, Method 2320B) and hardness (APHA, Method 2340A) were measured by titration.

Particle Counts

A Multiziser 3 (Beckman Coulter, Miami) was used to size particles. Particles suspended in an electrolyte solution (Isotone II, Beckman Coulter, Miami) are drawn through an aperture with electrodes on the sides that result in increased resistance, when current is applied, proportional to the actual volume of the particle. Distributions of counts, count per milliliter (μm/mL) or volume per milliliter (μm^3/mL) were obtained as a function of particle diameter.

Table 1. Experimental Design Used for Coagulation Experiments

Trial number	Coagulant dose (ppm alum)	Initial pH value	Spore concentration (cfu/mL)	Clay concentration (NTU)
1	0,10,20,30,40,60,80	5.0	3×10^4	0
2	0,10,20,30,40,60,80	6.8	3×10^4	0
3	0,10,20,30,40,60,80	8.2	3×10^4	0
4	0,10,20,30,40,60,80	5.0	3×10^4	5
5	0,10,20,30,40,60,80	6.8	3×10^4	5
6	0,10,20,30,40,60,80	8.2	3×10^4	5
7	0,10,20,30,40,60,80	8.2	3×10^4	10

Experimental Design

The research tasks were divided into two phases. Phase I determined conditions to aggregate disperse *B. subtilis* spores and spores cosuspended with clay (terminology for spores that are suspended with clay particles), while Phase II focused on the UV inactivation of suspended and aggregated systems from Phase I.

Phase 1—Conditions for Aggregation Tests

The experimental matrix used for coagulation experiments is presented in Table 1. Coagulation and flocculation experiments were performed at bench scale with a standard jar test apparatus using four 1 L beakers. Concentrated alum $[Al_2(SO_4)_3\times14H_2O]$ obtained from the water treatment plant was used to prepare alum stocks. Different quantities of freshly prepared alum were added to each jar (0–80 ppm alum), mixed at 100 rpm for 2 min, reduced to 30 rpm for 20 min, and then settled for 30 min. After settling, the supernatant was analyzed for pH, turbidity, conductivity, absorbance, particle size, particle volume, surface area, mean diameter, TOC, zeta potential, and spore count. The ideal alum dose for coagulation experiments refers to conditions under which the lowest turbidity values in the supernatant were obtained.

Phase 2—UV Irradiation Experiments

The UV disinfection experimental design allowed for comparison of the UV fluence-response results of spores either cosuspended or aggregated with clay particles, or with other spores. The matrix for UV experiments was performed at ideal conditions for aggregation as determined during Phase I coagulation experiments. Simulated DW was spiked with 3×10^4 cfu/mL of spores and with or without addition of 5 NTU clay, as illustrated in Fig. 1:

1. Jar A—no alum added, rapid and slow mixing without settling (Jar A1 or A2, Fig. 1);
2. Jar B—alum added at ideal conditions, rapid and slow mixing without settling (Jar B1 or B2, Fig. 1); and
3. Jar C—ideal alum conditions, rapid and slow mixing with settling.

Suspensions from Jars A and B were exposed to UV fluence of 0, 5, 10, 20, 30, 40, 50, and 60 mJ/cm^2, while the supernatant in Jar C was sampled for those exposures. After UV exposures, the spores were enumerated before and after physical separation techniques such as blending to assess the extent of particle association achieved (Parker and Darby 1995). Recovery of spore count by vortex mixing of the aggregate for 1 min with known control spore concentration (3×10^4 cfu/mL) was performed to verify that blending was sufficient to release spores from the spore–spore or spore–clay aggregates.

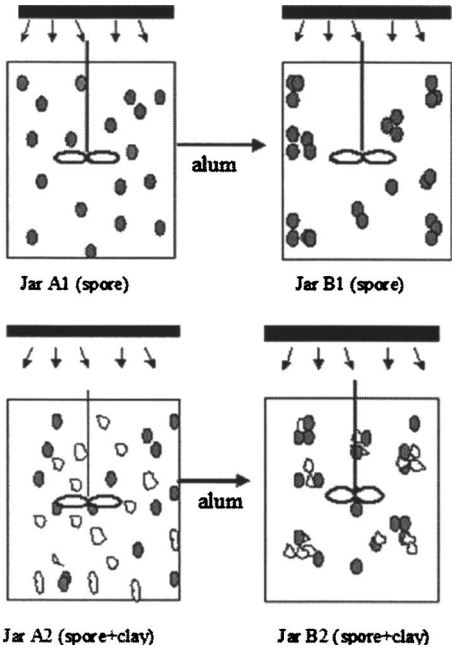

Fig. 1. Schematic representations of suspensions of dispersed and aggregated spore systems exposed to UV irradiation. Jar A1 represents suspension of disperse spores; Jar A2 represents suspension of disperse spores cosuspended with clay; Jar B1 represents suspension of aggregated spores; Jar B2 represents suspension of spore–clay aggregate.

Low-Pressure UV Irradiation System and Radiometry

A quasiparallel beam bench scale UV apparatus consisted of four 15 W low-pressure mercury vapor germicidal lamps (ozone-free, General Electric #G15T8) emitting nearly monochromatic UV radiation at 253.7 nm that was directed through a circular opening to provide incident radiation normal to the surface of the test suspension. These lamps do not emit at 185 nm due to the quartz used. Incident UV irradiance (mW/cm^2) was measured with a radiometer and a UV detector (International Light IL1400, Newburyport, Mass., SEL 240 detector) that had been factory calibrated, traceable to National Institute of Standards and Technology (NIST) standards.

UV Fluence Determination and Exposures

The measured incident irradiance at the surface of the test liquid was corrected for nonhomogeneity of irradiation across the surface area of the Petri dish to provide the average incident irradiance. The average irradiance in the mixed suspension was determined mathematically from an integration of the Beer–Lambert law over the sample depth, accounting for UV absorbance of the test suspension and incident average irradiance (Morowitz 1950). UV absorbance was measured by UV-vis spectrophotometer (Varian Model Cary 100BIO, Victoria, Australia). Exposure times were calculated by dividing the desired UV fluence by the average UV irradiance. Ten milliliter volumes of sample placed in 60 mm diameter irradiation vessels with a microstirrer resulting in a sample depth of 4.53 mm were irradiated

Table 2. Spore Count as Function of Settling Time

Time (min)	Spore count
0	5.3×10^5
30	5.4×10^5
60	5.9×10^5
240	5.9×10^5

using the bench scale UV system. Each exposure was performed in duplicate at UV fluence ranging from 0 to 60 mJ/cm^2.

Scanning Electron Microscopy

Scanning electron microscopy (SEM) was utilized to visualize the aggregates. The samples for SEM were fixed with 2% (wt/volume) glutaraldehyde for 1 h. Spore samples were collected by filtration with 0.22 and 3 μm polycarbonate filters (Millipore, Bedford, Mass.) or by absorbance to a poly-l-lysine coated cover slip in a humid chamber for 30 min (Becton-Dickinson Biocoat Cellware). Subsequently the samples were dehydrated through a graduated series of 30, 50, 75, and 100% (twice) ethanol solution. Following dehydration, samples were transferred to the critical point dryer, mounted on aluminum stub, coated with gold–palladium alloy by using a sputter coater, and viewed with a SEM (Cambridge S200). The SEM is equipped with a Kevex 7000 energy dispersive X-ray (EDX) analyzer. The elemental analysis of the aggregates was carried out qualitatively by EDX microanalysis. Samples for EDX analysis were coated with carbon for the elemental analysis.

Data Presentation

Mean concentration [colony forming units/milliliter (cfu/mL)] of spores spiked in suspension without UV exposure was taken as the initial concentration, N_0. Duplicates of 10 mL samples of spore–water mixed suspension were irradiated under predetermined UV fluence. Each duplicate was serially diluted and plated three times per UV fluence. All the data fields from each repetition were organized in two columns; one for fluence and one for spore concentration (cfu/mL). The mean concentration per fluence (N_d) and standard deviation from all data fields were summarized. The $\log_{10}$ transformation for N_0/N_d was plotted as a function of the UV fluence (H). Regression analysis and 95% confidence interval (CI) was determined on all the data fields used to fit the linear sections of the log inactivation curve. The linear curve was described by the following equation:

$$\log_{10}\left(\frac{N_0}{N_d}\right) = k \cdot H \tag{1}$$

The fluence based inactivation rate constant (k) was determined for each experimental run.

Results and Discussion

Control Testing

Free settling of *B. subtilis* spores was measured by placing the spore suspension into a 100 mL glass cylinder and taking 1.5 mL samples at 2 cm below the surface of the sample at times of 0, 30, 60, and 240 min. As shown in Table 2, the concentration of the spores was consistent over time indicating that monodispersed spores do not settle. This testing is important since removal of spores at the settling stage of the jar testing should be due only to the aggregation (with alum) and not due to settling of individual spores or autoaggregation (without alum).

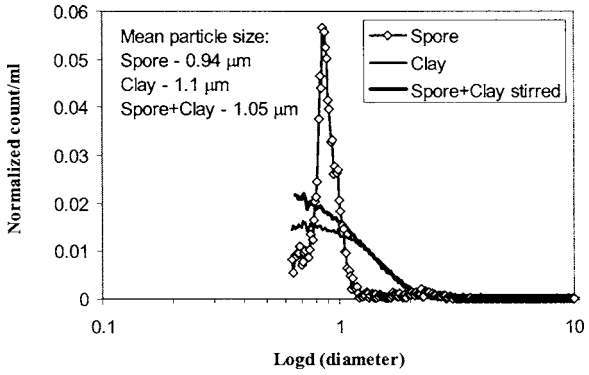

Fig. 2. Particle size distribution of *Bacillus subtilis* spores and montmorillonite clay particles suspended in simulated drinking water

The next control test was performed by placing the spore suspension in a jar test apparatus without alum addition at similar mixing conditions as the coagulation experiments. This test determined if collisions due to jar test conditions resulted in autoflocculation of spores. Without physical removal by settling, autoflocculation of spores remaining in the supernatant can reduce spore titer. This can occur because each aggregate, made up of numerous formerly single disperse spores, will likely result in one colony when enumerated on agar medium. To avoid this artifact, physical separation techniques were employed to disperse any aggregate that might not have settled. Vortex blending of the suspended aggregates with conditions tested in the "Methods" section was sufficient to release spores. Consequently, spore counts represent actual removal and are not an artifact of lower counts grown on the plate due to autoflocculation of spores. The concentration of spores in the supernatant after mixing and settling was similar to initial concentration, indicating minimization of settled autoflocculation. Even if a small percent of spores had autoflocculated and remained suspended, it did not have an effect on spore count or on particle size distribution and therefore could not be examined.

The third control test determined the conditions to separate the individual spores from clay particles after aggregation in a jar tester. The same spore counts were obtained in the supernatant for a spore and clay cosuspension in a jar tester that was further aggregated with alum (without settling). Therefore vortex blending is also sufficient to release the individual spores entrapped in an aggregate. Since spores and clay particles have similar mean particle size (Fig. 2) individual spores cannot be differentiated in solution by filtration after disturbing the aggregate.

Previous research showed that turbidity interferes with coliform counts of unfiltered surface waters as particles mask coliform counts on membrane filters (LeChevallier et al. 1981), therefore the effect of turbidity on spore counts was also examined. High turbidity of up to 10 NTU did not mask spore counts on plate count agar used for enumeration of spores. The aggregates formed in the jar test were apparently weak as gentle shaking destroyed most of the larger aggregates into smaller ones. Control of disaggregation was performed by sampling aggregates under low suction with a wide opening (inlet of 25 mL pipette after removal of the cotton stopper) and maintaining an

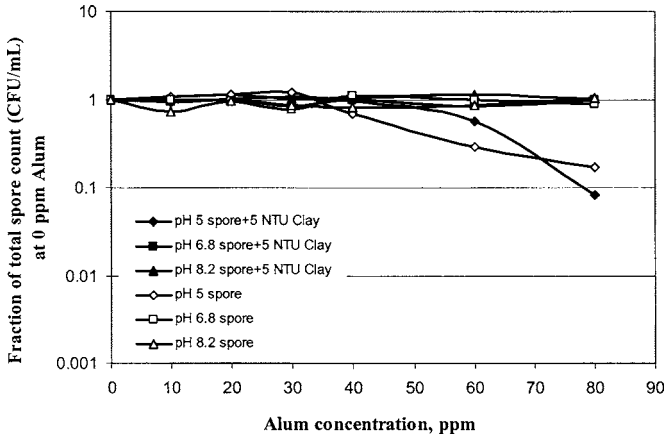

Fig. 3. Impact of alum on aggregation of spores and spores associated with clay particles, at different pH values, as measured by spore concentration in supernatant after settling

aggregate suspension under constant mixing. Upon sampling for any measurement, aggregates had probably disaggregated to a certain extent across all samples.

Conditions for Aggregation Tests

The impact of alum on aggregation efficiency of spores and spores cosuspended with clay particles as measured in supernatant after settling is illustrated in Fig. 3. Spore count in the supernatant after alum addition relative to the initial spore count of the uncoagulated sample indicates the degree of aggregation. At pH 6.8 and 8.2 spores did not aggregate, even up to alum dose of 80 ppm. Addition of 5 or 10 NTU clay particles to the water matrix did not affect the aggregation at those pH values. At pH 5 and 60 ppm alum, spores and added clay particles aggregated to a certain extent but the spores also aggregated by themselves, indicating the clay did not considerably impact aggregation under these conditions. However, at 80 ppm alum, addition of clay to the water matrix enhanced the extent of aggregation by more than 90%. Addition of alum to jar test experiments had a slight effect on the solution pH at pH 6.8 and 8.2, while at pH 5 the solution pH reduced to 3.6, as it was difficult to maintain a buffered solution (Table 3). The alkalinity of 3 mg/L as $CaCO_3$ was completely consumed at ideal conditions for aggregation. Ideal alum doses of 60–80 ppm are high and not typical of natural waters, but likely due to the nature of the simulated DW used. Although waters at pH 5 are not representative of typical surface waters, high alum dose and pH adjustment to a pH of 5–6 during coagulation was shown to be effective for waters with high alkalinity for removal of TOC and *Cryptosporidium* in water (Krasner and Amy 1995; States and Tomko 2002). In this study the lower pH conditions for aggregation were necessary to achieve the desired particle association via coagulation.

pH for coagulation is partly dependent upon anions present in solution such as sulfate, chloride, and phosphates that can form complexes with the metal ion and may compete with the OH^- ions on the coordinative sites of the aluminum cation and results in lower pH for ideal coagulation (Stumm and Morgan 1962). This may explain why coagulation of simulated waters with high phosphate concentrations occurred at lower pH than is typical for alum coagulation. Another explanation is that in the simulated drinking water with high alkalinity at pH 6.8 and 8.2, the flocs of aluminum hydroxide were produced rapidly and were inefficient for the coagulation process, whereas at pH 5 with lower buffer capacity, clay particles could be destabilized via the efficient hydroxide sols that develop slowly. Also, under acidic conditions, aggregation of clay particles is enhanced due to a decrease in repulsion (Wen et al. 1997) as was likely in the pH 5 simulated waters. However, examining the impact of changing the composition of the simulated DW water on coagulation efficiency was not within the scope of this study.

Particle Characteristics of Cosuspended and Aggregated Systems

At ideal coagulation conditions, the supernatant after settling was analyzed for spore concentration (cfu/mL), particle count/milliliter, particle volume/milliliter and particle surface area/milliliter. The fraction relative to 0 ppm alum for each parameter was calculated as shown in Fig. 4. The goal was to investigate whether the particle parameters as measured by the particle size analyzer, could be correlated to spore removal (cfu/mL). Particle parameters measured in the supernatant after floc settling followed a parallel removal pattern to that of the spore count (cfu/mL) suggesting that particle parameters can be used to indicate aggregation of spores with alum.

A similar test was conducted on simulated water with spiked spores and added clay particles to achieve a turbidity of 5 NTU (Fig. 5), as this is the maximum allowed turbidity of unfiltered drinking water systems prior to disinfection (40 CFR 141.71, USEPA). When clay particles were added, removal of spores did not parallel particle removal. At a dose of 80 ppm alum, 65% TOC removal and 90% removal of spores was observed, however more than 99% of total particle count, total particle volume, and

Table 3. Impact of Alum on Zeta Potential of Spores Aggregated with Clay Particles

Alum concentration (ppm)	Zeta potential (mV)	pH	Particle count sup[a]	Particle size sup[a] (μm)	Particle size agg[b] (μm)	Turbidity (NTU)	Conductivity (μS/cm)
0	−21.9±1.6	5.0	4.50×10^7	1.12	1.04±0.34	5.08	630
10	−21.7±2.1	4.6	4.53×10^7	1.11	—	8.15	640
20	−22.5±2.6	4.3	4.51×10^7	1.11	—	11.9	650
30	−18.8±1.6	4.1	4.48×10^7	1.11	—	13.7	670
40	−13.5±0.9	4.0	8.33×10^7	1.04	—	17.8	660
60	−10.9±1.5	3.8	2.42×10^7	0.96	—	6.29	700
80	~0±2	3.6	5.11×10^5	0.92	2.47±0.35	0.46	740

[a]Average particle size of the system in the supernatant.

[b]Average particle size of the aggregated prior to settling.

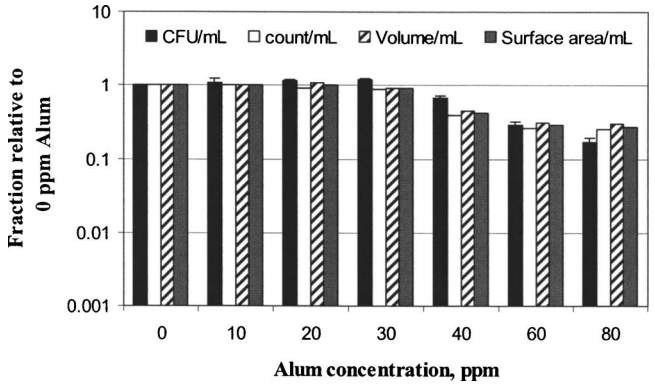

Fig. 4. Impact of alum on concentration and particle characteristics of aggregated spores (without clay particles), as measured in supernatant after settling. Fraction of each characteristic measured (spore count, particle count, volume or surface) is measured relative to that certain characteristic prior to alum addition. Counts in supernatant are residual counts of spores or particles left after settling.

total particle surface area were removed, indicating enhanced clay removal compared to spores. It was hypothesized that not all the aggregates formed upon addition of clay were homogeneous and the ratio of the number of spores to clay particles in each aggregate was different, resulting in differing removal rate between the spore and particle parameters.

Particle counts and turbidity are not reliable indicators for removal of *Cryptosporidium* due to the low concentration of *Cryptosporidium* compared to the concentration of other particles (Edzwald and Kelley 1998). Clay particle counts per milliliter are 2 orders of magnitude larger than spore count per milliliter (10^7 compared to 10^5), for a given particle size, as analyzed with the particle size analyzer (Table 3). Therefore within a spore–clay aggregate, more clay particles are removed compared to spores, thus aggregates contain uneven amounts of spores and clay particles per aggregate.

The mean particle size of spores is $\sim$1 μm, similar to clay particles, however spores exhibit a narrow particle distribution compared to the broad distribution of clay particles (Fig. 1). The particle size analyzer does not allow measurements below the detection limit ($<$0.6 μm). Due to the shape of the distribution curve for the clay particles, it is assumed that particles in the

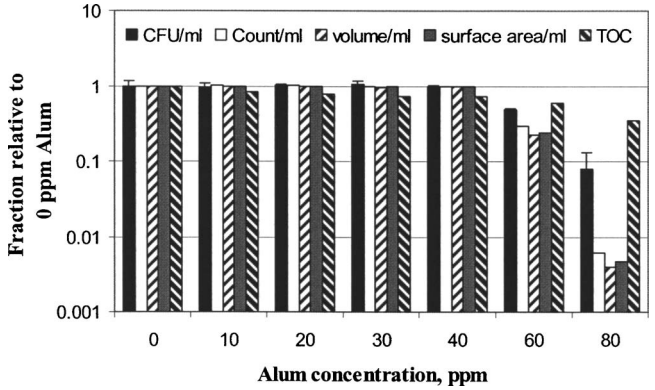

Fig. 5. Impact of alum on concentration and particle characteristics of spores aggregated with clay particles, as measured in supernatant after settling

Table 4. Calculated Concentration of Spore–Clay Aggregates over Different Alum Doses

Alum dose (ppm)	Spores in suspension (0 ppm alum) (cfu/mL)	Spores in supernatant (cfu/mL)	Calculated aggregated spores (cfu/mL)
10–40 (avg)	28,300±4,900	29,700±2,600	0
60	28,300±4,900	15,900±300	12,400
80	28,300±4,900	2,600±300	25,700

lower-scale range exist but are not accounted for in the particle analysis. Spores and clay particles have similar mean particle size, therefore shielding of UV light by the clay particles is probably not the dominant mechanism of spore protection from UV. Because the concentration of clay particles is more than 2 orders of magnitude higher than spore concentration, there is a statistical likelihood of having more clay particles in an aggregate than spores, thus providing spores protection from UV.

Clay particles are irregular in shape, however the assigned particle size is an average size and the size differences are illustrated in the distribution. Clay particles have unique chemical, mineralogical, and structural properties that may differ compared to other particles in natural waters, including possibly other clays in natural waters. Na–montmorillonite was selected for this study due to its high sorption capacity. Montmorillonite is a layered 2:1 clay that has internal structure allowing expansion and contraction with exchangeable ions within opposing layers. It has tetrahedral sheets held together weakly, capable of expanding and having both internal and external surface area. The preferential content within an aggregate is further complicated, as spores can be relatively hydrophobic (Doyle et al. 1984) and other characteristics as shape and surface charge of spores compared to clay particles may affect the ratio or location of spores to clay particles within an aggregate.

Table 4 presents the theoretical concentration of spores in spore–clay aggregates, with different alum doses. The extent of spores aggregated was calculated by the difference in the spore concentration before and after settling due to aggregation. An alum dose of 60 ppm resulted in 44% of spores aggregated and at an alum dose of 80 ppm 91% of spores aggregated. The turbidity of the solution with 3×10^4 cfu/mL of spores (without clay particles) was very low at a value of 0.01 NTU, thus clay particles were the major contributors to the simulated water turbidity of 5 NTU. The supernatant (after settling of spore–clay aggregates) at ideal conditions for aggregation had a turbidity of 0.5 NTU compared to initial turbidity of 5 NTU, therefore turbidity measurements indicate 90% particle removal, which matches the 90% removal as measured by spore concentration (Fig. 5 and Table 3). However turbidity may not be the best true measure of particle removal. Adin (1999) concluded that optimum removal of submicron particles upon alum coagulation was represented by turbidity measurement while removal of particles larger than 1 μm was measurable best through particle size analyzers. Bell Ajy et al. (2000) suggested using particle counts and not turbidity to evaluate improved coagulation processes. Rice et al. (1996) emphasized that turbidity is a reliable measure of particle removal when source water turbidity is above 5 NTU, whereas particle count is a more reliable measure in less turbid waters. Because data for removal of count/milliliter, volume/milliliter and surface area/milliliter were similar (Figs. 4 and 5), it is only necessary to measure one of these parameters. Therefore it is suggested to compare the normalized count/milliliter and colony forming unit/milliliter when efficiencies in removal are evaluated. Rice et al.

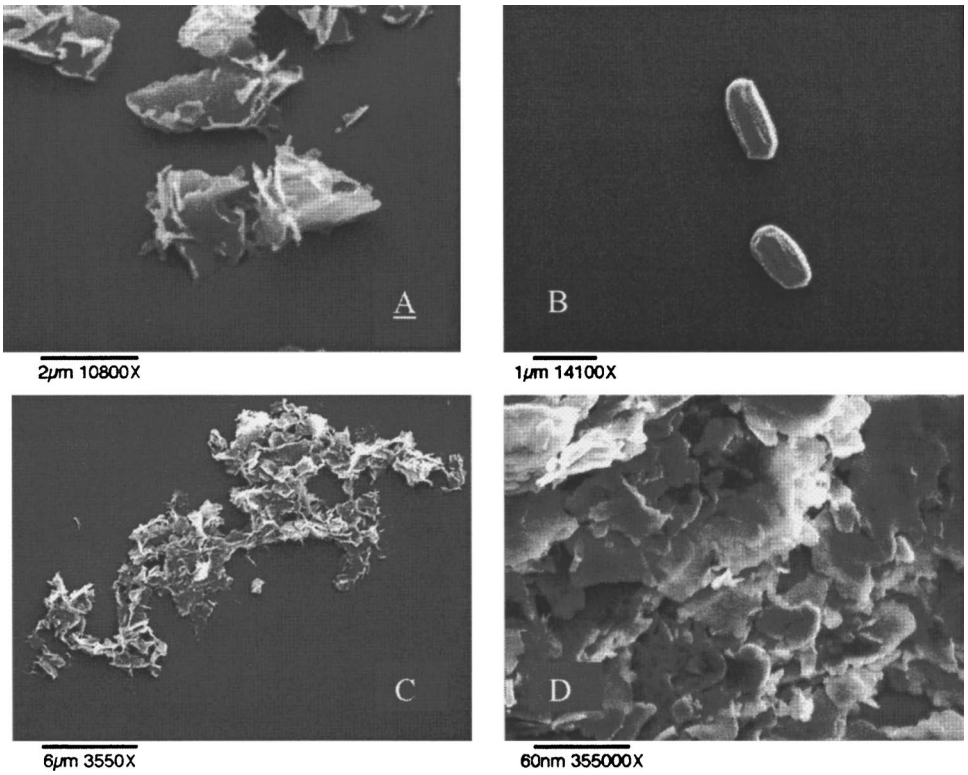

Fig. 6. Scanning electron microscopy images of dispersed and aggregated clay particles, and dispersed spores. Images of dispersed clay particles (A), dispersed spores (B), clay self-aggregated with irregular shapes (C), and closeup of clay surfaces (D).

(1996) found that for some water utilities, spore removal corresponded to particle removal and for others, spore removal was less than particle removal, and therefore spores could be used as a conservative indicator of removal efficiency.

Scanning Electron Microscopy–Energy Dispersive X-ray Microanalysis

Fig. 6 illustrates scanning electron microscopy images of dispersed clay particles (A) and dispersed spores (B). Clays tend to self-aggregate with irregular shapes (C), with different surfaces observed on the clay particles for attachment (D). Because clay particles tend to self-aggregate, the accessible surface sites for aggregation of spores when alum is added to the system may change. Consequently this may affect the position of spores within the aggregate and the density of the aggregate, affecting the pathway of light through the aggregate and the extent of aggregation. Whether aggregates necessarily included clay particles was further analyzed by EDX microanalysis. Fig. 7 illustrates SEM images of clay–spore aggregates (A, E, and F), spore aggregates (C), and elemental analysis of the aggregates determined by EDX microanalysis (B and D). Various aggregate shapes and the alum polymeric coating of the particles were observed in SEM images. Sections of aggregates were analyzed by EDX and resulted in two types of scans: one with the elements aluminum (Al) and sulfur (S), and the other with additional elements as silicon (Si), iron (Fe), zinc (Zn), and potassium (K). Clearly, Al and S originate from alum and correspond to spores aggregated by alum (C) since control testing of spores coated with alum show elemental analysis of Al and S, while the other elements originate from clay and correspond to clay–clay or clay–spore aggregates. This strengthens the hypothesis of nonhomogenous aggregate composition. In some of the aggregates it was not obvious whether spores were included in the aggregate as the alum coating masked the distinct shape of the spores

Adin (1999) found that differences observed in particle shape correspond to different origins of the wastes and are reflected in the particle surface chemical composition as detected by SEM-EDX analysis. For instance, their results pointed out that particles from an open reservoir are dominated by Si, whereas particles from an activated sludge plant are dominated by Cl, Si, and Ca. Therefore EDX microanalysis can be an important tool to determine the origin of particles via the distribution of elements in different flocs of water treatment after coagulation.

Zeta Potential of Aggregated Spores

The electrostatic surface properties as measured by zeta potential may influence the complex mechanisms by which microorganisms are associated with suspended particles. Although zeta potential is not a direct measure for particle removal, it can be used to determine the optimized coagulation dose (Rice et al. 1996). The zeta potential of spores aggregated with clay particles at pH 5 and below is presented in Table 3. Charge neutralization as measured by zeta potential was achieved at a dose of 80 ppm alum. Spores and clay particles carry a negative charge and are attracted to positively charged aluminum ions and hydroxides that neutralize the particle charge, allowing for flocculation via intermolecular forces. Zeta potential measurements paralleled the removal of particle parameters as 100% charge neutralization was reached after dose of 80 ppm alum. The flocs viewed during the zeta potential measurements were larger at a dose of 80 ppm alum, suggesting a correlation between alum dose and aggregate size. The zeta potential without alum addition was −22 mV thus

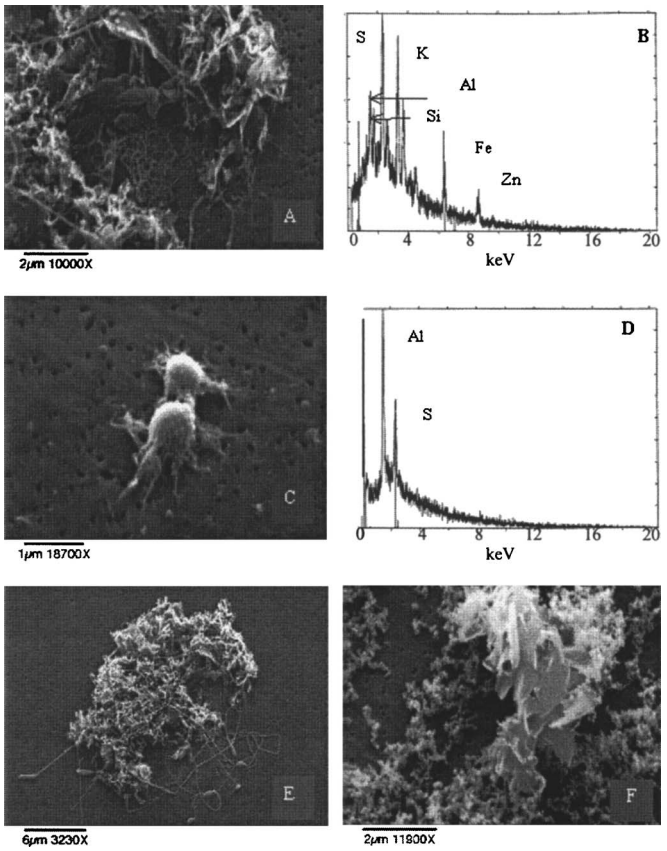

Fig. 7. Scanning electron microscopy images and energy dispersive X-ray (EDX) analysis of spore and spore–clay aggregates by alum. Clay–spore aggregates (A, E, and F), spore aggregates (C), and EDX microanalysis (B and D) for elemental analysis of aggregates.

giving a stable dispersion in solution at pH 5. Zeta potential of clay particles suspended in simulated DW was -31.5 ± 3.3 mV, indicating that adding spores to the clay suspension decreased stabilization. Also removal of 90% of turbidity, 99% of particle counts, and a slight increase in conductivity was observed at 80 ppm alum (Table 3).

UV Irradiation Experiments of Spores

A base-line experiment was conducted to test whether pH had an affect on the UV inactivation of spores (Fig. 8). Variation in pH did not show a direct affect on the response of *B. subtilis* spores to UV, as the inactivation patterns were similar at all pH levels tested.

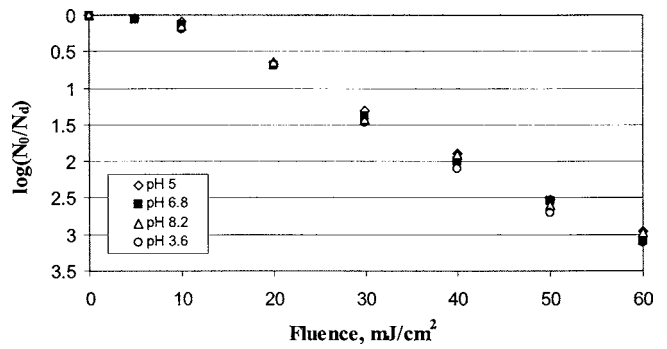

Fig. 8. Impact of pH on UV fluence–response curves of *Bacillus subtilis* spores

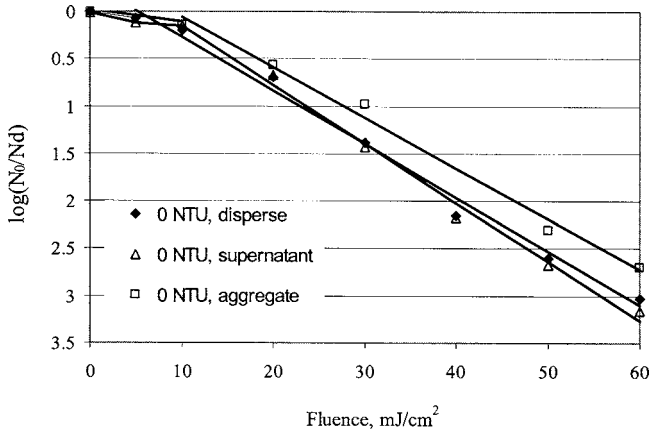

Fig. 9. Comparison of UV fluence–response of disperse spores (Jar A1, Fig. 1), spore aggregates (Jar B1, Fig. 1), and supernatant of spore system. Error bars represent ±standard deviation; 0 NTU aggregated system relates to upper line, while 0 NTU supernatant and 0 NTU disperse relates to two bottom lines.

The impact of suspended spores (Jar A1, Fig. 1) and aggregated spores (Jar B1, Fig. 1) on UV fluence–response curves of spores, at pH 5 (without clay) is illustrated in Fig. 9. The goal in this experiment was to determine if there were differences in UV inactivation between disperse (noncoagulated) spores in suspension and aggregated spores. A fluence of 30 mJ/cm^2 resulted in $\log_{10}$ inactivation of 1.12 and 1.4 for aggregated and suspended spores, respectively. These differences were nearly consistent for all UV fluences greater than 20 mJ/cm^2.

The inactivation rate constants (indicated by the slope) for suspended and aggregated spores (without clay) were 0.0594 and 0.0533 cm^2/mJ, respectively. The goal was to test if the shoulder and the first order regression lines of disperse spores and spores aggregated with alum measured by direct technique (Fig. 9) are represented statistically by the same or similar lines. Specifically it is important to assess whether similar slopes also have the same intercept, which indicates that the differences in the shoulder are also insignificant. The different combinations between shoulder and slopes are as follows: (1) both treatments (disperse versus aggregated, direct) with same slopes and intercepts; (2) both treatments with same slopes however with different intercepts; and (3) treatments are with different slopes and intercepts. The analysis of covariance (ANCOVA) method can be used to capture the interaction of the first order regression slope with a main effect (Sall et al. 2001) such as UV fluence with each treatment. In this study, this method is accomplished by introducing the interaction between log inactivation of spores and UV fluence with each treatment which is the main effect. The P value for the interaction is marginally significant at fluence levels of 10–60 mJ/cm^2 [$F(1,32)=3.6683$; $P=0.0654$] indicating that the difference in inactivation rate constants between the suspended and aggregated spores is not highly significant. The fluence response curve of the residual spores in the supernatant of the aggregated spore suspension and the UV fluence–response curve of the suspended (nonaggregated) spores were virtually identical.

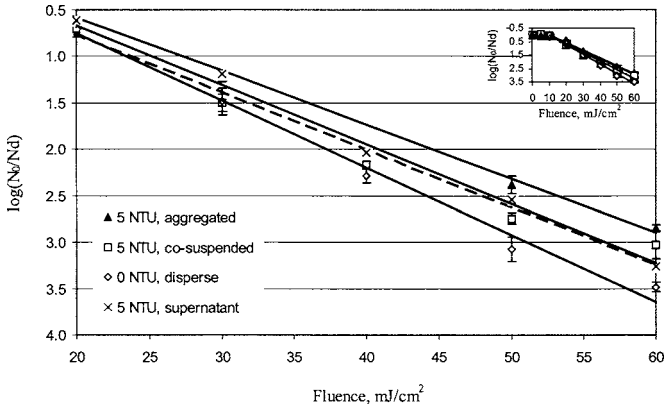

Fig. 10. Comparison of UV fluence–response of spores cosuspended with clay (Jar A2, Fig. 1), spore–clay aggregates (Jar B2. Fig. 1), disperse spores (Jar A1, Fig. 1), and supernatant of spore–clay system. Error bars represent the ±standard deviation (SD); 5 NTU aggregated system relates to upper line, 5 NTU cosuspended and 5 NTU supernatant relates to two middle lines, while 0 NTU disperse system relates to bottom line.

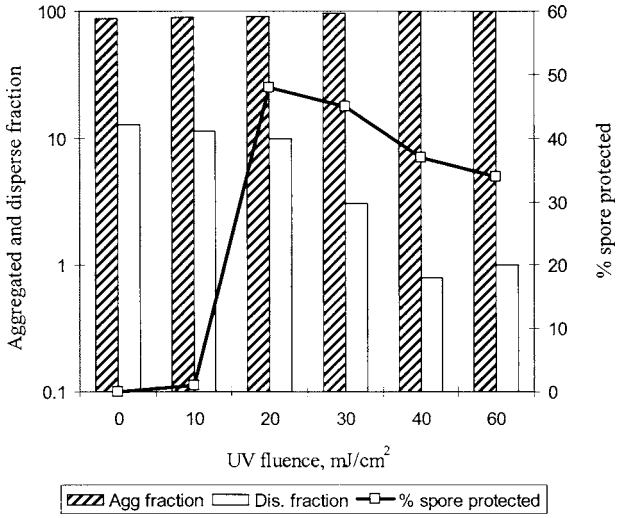

Fig. 11. Fraction of aggregated spores, dispersed spores in logarithmic scale (left *Y*-axis) and percent of spores protected from UV irradiation (right *Y*-axis). Basic system is comprised of spores with addition of 5 NTU clay particles either cosuspended or aggregated. All data from conditions at pH 5 and 80 ppm alum.

UV Irradiation Experiments of Spores and Clay Particles

Three different treatments were examined with an identical concentration of spores and clay particles. The impact of spores cosuspended with clay particles (Jar A2, Fig. 1), spore–clay aggregates (Jar B2, Fig. 1), and the supernatant of spore–clay aggregates after settling on UV fluence–response curves of spores, is illustrated in Fig. 10. A fluence of 30 mJ/cm^2 resulted in $\log_{10}$ inactivation of 1.24 and 1.5 for aggregated and suspended spores, respectively. The inactivation rate constants (slopes) for suspended and aggregated spores (with clay) were 0.0617 and 0.0579 cm^2/mJ, respectively. The ANCOVA model showed that the P value for the interaction was not significant at fluence levels of 10–60 mJ/cm^2 [$F(1,32)=3.6683$; $P=0.1631$]. However the microbial counts for the clay and spore suspended system at fluence of 60 mJ/cm^2 were close to the detection limit leaving these data suspect. When the fluence of 60 was omitted from the statistical analysis, the P value for the interaction between fluences of 10 and 50 mJ/cm^2 was found to be statistically significant [$F(1,30)=9.3153$; $P=0.0047$], indicating that the slopes are different and the difference between the inactivation rate constants for the suspended and aggregated spores when clay particles are added to the system is highly significant. Like in the aggregated system without clay addition, the fluence–response curve of the residual spores in the supernatant of alum treated spore–clay waters and the UV fluence–response curve of the spores suspended with clay particles were virtually identical. In comparison, disperse spores are UV inactivated to a greater extent and less protected from UV irradiation. UV inactivation of aggregated spores (Fig. 9) or aggregates of spores associated with clay particles (Fig. 10) indicate that spores in an aggregate are protected from UV with or without clay addition. The difference in the counts between dispersed and aggregated spores indicates that particle-associated spores in the water samples are being shielded from UV light.

The fraction of aggregated spores, dispersed spores, and spores protected from UV irradiation with addition of 5 NTU clay particles is presented in Fig. 11. The supernatant indicates the fraction of dispersed nonsettled spores remaining after the aggregates settled in the jar, assuming all aggregates settled. The aggregated system consists of spore–spore aggregates, spores–clay aggregates, and nonaggregated dispersed spores. The percent of true spore aggregates that are protected from UV irradiation was computed by the following:

1. The supernatant indicates the fraction of dispersed nonsettled spores remaining after the aggregates settled in the jar, assuming all aggregates settled.
2. The aggregated system consists of spore–spore aggregates, spores–clay aggregates, and nonaggregated dispersed spores.
3. The dispersed fraction is the number of spores in supernatant at each UV dose divided by the total number of spores in suspension prior to any aggregation. The aggregated fraction is the total spore count minus the dispersed count divided by the total count.
4. The percent of spores protected from UV irradiation was computed by the difference between the fraction of surviving spores in the spore–clay aggregated system and the fraction of surviving spores in the nonaggregated spore–clay system for all UV fluence levels. The fraction herein is relative to the count obtained at dose zero.

Recall the spores in the aggregated system were counted by dispersing the aggregate and thus measuring the total number of culturable spores within an aggregate. Based on this analysis, no inactivation of spores is observed up to fluence of 10 mJ/cm^2 since 0% of spores are protected from UV at the shoulder region of the spores, which is obvious. Approximately 30–50% of spores in the aggregates are protected from UV light across a UV fluence increase from 20 to 60 mJ/cm^2, with a decrease in the percent of spores within an aggregate that are protected from UV as the UV fluence increases. This decrease is expected if the aggregates contain zones that allow penetration of UV light over prolonged UV exposure with increase in fluence (Emerick et al. 2000). In a denser aggregate, UV light may not penetrate the aggregate, and an increase in UV fluence can result in tailing; however tailing was not observed in this study

Since a maximum of 50% of the microbes in the aggregated

system are protected from UV light, it may be assumed that initially the free or dispersed spores (not aggregated with alum) are inactivated, whereas all the spores within aggregates are protected similarly from UV. However, previous research showed that different distribution curves for the UV intensity within the aggregates exist and depend on light-accessible pathways in the various aggregates and positioning of microbes in and on the aggregate (Emerick et al. 2000). Inactivation within aggregates may be a function of the time factor or of an intensity factor. This may be a case where time-dose reciprocity does not hold, and possibly the more aggregates are exposed to UV over time, the more likely that the exposure through a path in the aggregate would occur. Therefore inactivation of aggregated spores will possibly depend on both the location of spores in the aggregate, the existence of zones that allow a pathway for penetration of UV light, and the time factor. The inactivation function of the combined dispersed–aggregated spore system results in linear inactivation kinetics as presented in Figs. 9 and 10.

Spore–spore aggregates and spore–clay aggregates both protect spores from UV inactivation as compared to nonaggregated spores. Spores in the spore–clay aggregates at a fluence of 60 mJ/cm^2 reach about 2.8 log inactivation compared to about 2.6 log inactivation of spore–spore aggregates which is not a significant difference. The slight increase in protection may result from denser spore–spore compared to spore–clay aggregates or differences in UV irradiation scattering properties in and on the different aggregates. Tailing of the fluence–response curve of the spore aggregates should be expected at a certain UV fluence, assuming spores located at the core of the aggregate are constantly protected regardless of the fluence. The kinetics of spore inactivation is linear up to a high fluence of 60 mJ/cm^2 with no tailing, thus tailing is not expected to occur at all. Another explanation for the decreased inactivation kinetics of the aggregated system might be due to the scattering of UV irradiation by aggregates, not accounted for in the UV fluence determination. Scattering effects of suspended and aggregated systems are addressed in the companion paper (Part II) to this research.

Practical Considerations

Although previous studies investigating effects of particles in water on inactivation of microbes found little to no effect of particles on inactivation, these results were likely because true particle–microbe association was not obtained. Similar to wastewater systems, coagulation/flocculation in drinking water treatment does produce aggregated microorganisms that will be protected from UV disinfection. Thus, the presence of particles can affect inactivation of microbes in drinking water if those aggregates are not properly removed by filtration. Future work should examine the relationship between common water quality parameters such as particle size analysis, and the potential for disinfection protection due to particle association, as well as the impact of aggregation when other coagulants and polymers are used. In most cases, particle size data from the aggregates showed increase in mean size (Table 3), thus particle size analysis could be used for monitoring a system for particle association.

Conclusions

The following conclusions can be drawn from the research study:

1. Particle parameters as counts of particle, volume, and surface area per milliliter are reliable indicators for removal of bacterial spores, but not when clay particles are present in the system.
2. pH does not effect UV inactivation of spores spiked into a simulated water matrix.
3. Aggregate composition is nonhomogeneous with respect to the number of spore and clay particles within aggregates and with respect to the ratio of spores and clay particles among aggregates in the spore–clay system.
4. For the same UV fluence, spore–spore and spore–clay aggregates were less inactivated compared to spores suspended with clay particles.
5. Approximately 30–50% of the spores in aggregates are protected from UV irradiation, but the percent of spores within an aggregate protected from UV decreases with increase in fluence.

Acknowledgments

The writers gratefully acknowledge Professor Regina Sommer, Institute of Hygiene, University of Vienna, Vienna, Austria, for providing *Bacillus subtilis* spores for this research, and Professor Robert Bagnell, the University of North Carolina at Chapel Hill, who provided microscopic facilities and advice for aggregate imaging. They also thank the Ultraviolet Research Group at Duke University including Dr. Sharpless and Dr. Ormeci who assisted in this project. This research was funded by the USEPA Science to Achieve Results (STAR) Program, Grant No. R82-9012. At the time of this research, Dr. Mamane was a doctoral candidate in the Department of Civil and Environmental Engineering at Duke University.

Notation

The following symbols are used in this paper:

H = fluence;
k = fluence based inactivation rate coefficient determined;
N_d = concentration per fluence; and
N_0 = initial concentration.

References

Adin, A. (1999). "Particle characteristics: A key factor in effluent treatment and reuse." *Water Res.*, 40, 67–74.

American Public Health Association, American Water Works Association, Water Environment Federation (APHA, AWWA, WEF). (1995). *Standard methods for the examination of water and wastewater*, 19th Ed., Washington, D.C.

Averett, R. C., Leenheer, J. A., McKnight, D. M., and Thorn, K. A. (1994). "Humic substances in the Suwannee River, Georgia: Interactions, properties, and proposed structures." *USGS water-supply paper*. ⟨http://www.ihss.gatech.edu⟩

Bell-Ajy, K., Abbaszadegan, M., Ibrahim, E., Verges, D., and LeChevallier, M. (2000). "Conventional and optimized coagulation for NOM removal." *J. Am. Water Works Assoc.*, 92(10), 44–58.

Cairns, W., Sakamoto, G., Comair, C., and Gehr, R. (1993). "Assessing UV disinfection of a physico-chemical effluent by medium pressure lamps using a collimated beam and pilot plant." *Proc., Planning, Design and Operation of Effluent Disinfection Systems, Water Environment Federation Specialty Conf.*, WEF, Whippany, N.J.

Doyle, R. J., Nedjat-Haiem, F., and Singh, J. S. (1984). "Hydrophobic characteristics of *Bacillus* spores." *Curr. Microbiol.*, 10, 329–332.

Edzwald, J. K., and Kelley, M. B. (1998). "Control of *Cryptosporidium*: From reservoirs to clarifiers to filters." *Water Sci. Technol.*, 37(2), 1–8.

Emerick, R. W., Loge, F. J., Ginn, T., and Darby, J. L. (2000). "Modeling the inactivation of particle-associated coliform bacteria." *Water Environ. Res.*, 72(4), 432–438.

Emerick, R. W., Loge, F. J., Thompson, D., and Darby, J. L. (1999). "Factors influencing ultraviolet disinfection performance. II: Association of coliform bacteria with wastewater particles." *Water Environ. Res.*, 71(6), 1178–1187.

Krasner, S. W., and Amy, G. . (1995). "Jar-test evaluations of enhanced coagulation." *J. Am. Water Works Assoc.* 87(10), 93–107.

LeChevallier, M. W., Evans, T. M., and Seidler, R. J. (1981). "Effect of turbidity on chlorination efficiency and bacterial persistence in drinking water." *Appl. Environ. Microbiol.*, 42(1), 159–167.

Loge, F. J., Emerick, R. W., Thompson, D. E., Nelson, D. C., and Darby, J. L. (1999). "Factors influencing ultraviolet disinfection performance. I: Light penetration to wastewater particles." *Water Environ. Res.*, 71(3), 377–381.

Malley, J. P. (2000). "Engineering of UV disinfection systems for drinking water." *International Ultraviolet Association News*, 2(3), 8–12.

Morowitz, H. J. (1950). "Absorption effects in volume irradiation of microorganisms." *Science*, 111, 229–230.

Parker, J. A., and Darby, J. L. (1995). "Particle-associated coliform in secondary effluents: Shielding from ultraviolet light disinfection." *Water Environ. Res.*, 67(7), 1065–1075.

Passantino, L., Malley, J., Knudson, M., Ward, R., and Kim, J. (2004). "Effect of low turbidity and algae on UV disinfection performance." *J. Am. Water Works Assoc.*, 96(6), 128–137.

Qualls, R. G., Flynn, M. P., and Johnson, D. (1983). "The role of suspended particles in ultraviolet disinfection." *J. Water Pollut. Control Fed.*, 55(10), 1280–1285.

Rice, E. W., Fox, K. R., Miltner, R. J., Lytle, D. A., and Johnson, C. H. (1996). "Evaluating plant performance with endospores." *J. Am. Water Works Assoc.*, 88(9), 122–130.

Sall, J., Lehman, A., and Creighton, L. (2001). "Fitting linear models." *JMP start statistics*, 2nd Ed., Duxbury Thompson Learning, Pacific Grove, Calif., 305–328.

Sharpless, C. M., Page, M. A., and Linden, K. G. (2003). "Impact of hydrogen peroxide on nitrite formation during UV disinfection." *Water Res.*, 37(19), 4730–4736.

Sobsey, M. D., Fuji, T., and Hall, R. W. (1991). "Inactivation of cell associated and dispersed Hepatitis-A virus in water." *J. Am. Water Works Assoc.*, 83(11), 64–67.

Sommer, R., and Cabaj, A. (1993). "Evaluation of the efficiency of a UV plant for drinking water disinfection." *Water Sci. Technol.*, 27, 357–362.

Stagg, C. H. (1976). "Inactivation of solids associated virus by hypochlorous acid." Ph.D. dissertation, Rice Univ., Houston.

States, S. , and Tomko, R. J. (2002). "Enhanced coagulation and removal of *Cryptosporidium*." *J. Am. Water Works Assoc.*, 94(11), 67–77.

Stewart, M. H., and Olson, B. H. (1996). "Bacterial resistance to potable water disinfectants." *Modeling disease transmission and its prevention by disinfection*, C. J. Hurst, ed., Cambridge University Press, Cambridge, U.K., 140–192.

Stumm, W., and Morgan, J. M. (1962). "Chemical aspects of coagulation." *J. Am. Water Works Assoc.*, 54(8), 971–994.

Templeton, M. R., Andrews, R. C., Hofmann, R., and Whitby, G. E. (2003). "UV inactivation of floc-associated MS2 coliphage." *Proc., 76th Annual Water Environment Federation Technical Exhibition and Conf. (WEFTEC)*, WEF, Los Angeles.

Tombacz, E., Filipcsei, G., Szekeres, M., and Gingl, Z. (1999). "Particle aggregation in complex aquatic systems." *Colloids Surf., A*, 151, 233–244.

U.S. Environmental Protection Agency (USEPA). (2003). "Draft ultraviolet disinfection guidance manual." *EPA 815-D-03-007*, Office of Water, Washington, D.C.

Van Olphen, H. and Fripiat, J. J. (1979). *Data handbook for clay minerals and other non-metallic materials*, Pergamon, New York, ⟨http://www.clays.org⟩

Wen, H. J., Liu, C. I., and Lee, D. J. (1997). "Size and density of flocculated sludge flocs." *J. Environ. Sci. Health [C]*, 32(4), 1125–1137.